Eur. J. Biochem. **263**, 912–920 (1999) © FEBS 1999

Transferrins, the mechanism of iron release by ovotransferrin

Fadi Bou Abdallah and Jean-Michel El Hage Chahine

Institut de Topologie et de Dynamique des Systèmes, l'Université Denis Diderot Paris 7 associé au CNRS, Paris, France

Iron release from ovotransferrin in acidic media ($3 < pH < 6$) occurs in at least six kinetic steps. The first is a very fast (≤ 5 ms) decarbonation of the iron-loaded protein. Iron release from both sites of the protein is controlled by what appear to be slow proton transfers. The N-site loses its iron first in two steps, the first occurring in the tenth of a second range with second order rate constant $k_1 = (2.30 \pm 0.10) \times 10^4$ M^{-1}·s^{-1}, first order rate constant $k_{-1} = (1.40 \pm 0.10)$ s^{-1} and equilibrium constant $K_{1a} = (60 \pm 6)$ μM. The second step occurs in the second range with a second order rate constant $k_2 = (5.2 \pm 0.15) \times 10^3$ M^{-1}·s^{-1}, first order rate constant $k_{-2} = (0.2 \pm 0.02)$ s^{-1} and equilibrium constant $K_{2a} = (39 \pm 5)$ μM. Iron is afterward lost from the C-site of the protein by two different pathways, one in the presence of a strong Fe(III) ligand such as citrate and the other in the presence of weak ligands such as formate or acetate. The first step, common to both paths, is a slow proton uptake which occurs in the tens of second range with a second order rate constant $k_3 = (1.22 \pm 0.03) \times 10^3$ M^{-1}·s^{-1} and equilibrium constant $K_{3a} = (1.0 \pm 0.1)$ mM. In the presence of citrate, this step is followed by formation of an intermediate complex with monoferric ovotransferrin; stability constant $K_{LC} = (0.435 \pm 0.015)$ mM. This last step is rate-controlled by slow proton gain which occurs in the hundred second range with a second order rate constant $k_4 = (1.05 \pm 0.05) \times 10^4$ M^{-1}·s^{-1}, first order rate constant $k_{-4} = (1.0 \pm 0.1) \times 10^{-2}$ s^{-1} and equilibrium constant $K_{4a} = (0.95 \pm 0.15)$ μM. In the presence of a weak iron(III) ligand such as acetate or formate, formation of an intermediate complex is not detected and iron release is controlled by two final slow proton uptakes. The first occurs in the hundred to thousand second range, second order rate constant $k_5 = (6.90 \pm 0.30) \times 10^6$ M^{-1}·s^{-1}. The last step occurs in the thousand second range. Iron release by ovotransferrin is similar but not identical to that of serum-transferrin. It is slower and occurs at lower pH values. However, as seen for serum-transferrin, it seems to involve the protonation of the amino acid side-chains involved in iron co-ordination and perhaps those implicated in interdomain H-bonds. The observed proton transfers are, then, probably controlled by the change in conformation of the binding lobes from closed when iron-loaded to open in the apo-form.

Keywords: transferrin; ovotransferrin; iron metabolism; stopped-flow.

Transferrins constitute the most important iron regulation system in vertebrates and some invertebrates, such as worms and insects [1]. Soluble transferrins, such as serum-transferrin, lactoferrin and ovotransferrin, are glycoproteins consisting of a single chain of about 700 amino acids and 80 kDa. These proteins have very similar 3D structures and are all bilobal. Each lobe contains an iron complexation cleft, in which the metal is co-ordinated to the side-chains of four amino acid ligands and a synergistic carbonate or bicarbonate [2–5]. This synergistic anion is absolutely essential for the interaction of these proteins with the metal [6–9]. The affinities of transferrins for iron are extremely high (in the 10^{20} M^{-1} range) [1]. These high values are absolutely required to solubilize Fe(III) in neutral physiological media and can prefigure the functions of transferrins in the metabolism of iron [10]. Indeed, these proteins possess at least two metabolic functions: (a) iron transport and/or (b) scavenging. In mammals, serum-transferrins transport iron from neutral biological fluids to the cytoplasm by receptor mediated endocytosis. Iron is then released inside the cell in acidic endosomes (pH ≈5.5). The protein is afterwards recycled back to the extracellular medium [11]. In contrast, lactoferrins sequester iron in biological fluids to avoid its use by microorganisms [1]. In birds, ovotransferrins insure this double function by being both iron scavenging and iron delivery agents [4].

In two previous articles [12,13], we examined the mechanism of iron release from transferrin in acidic media [Mechanism 1, Eqns (1–8)].

Correspondence to J.-M. El Hage Chahine, Institut de Topologie et de Dynamique des Systèmes, Université Paris 7 – CNRS, 1 rue Guy de la Brosse, 75005 Paris, France. Fax: + 33 1 4427 6814, Tel.: + 33 1 4427 6807, E-mail: chahine@paris7.jussieu.fr

Abbreviations: sT′Fe, serum holo–transferrin in interaction with bicarbonate; sT'_NFe and sT'_CFe, the N-site and C-site of iron-loaded serum-transferrin, respectively, in an unknown state of charge and protonation; HsT_NFe, H_2sT_NFe, H_3sT_NFe, H_2sT_N, H_3sT_N, H_3sT_CFe, H_3sT_CFeL, H_3sT_C and H_4sT_C, the different prototropic species in an unknown state of charge and protonation detected after bicarbonate loss during iron release by the N-site and C-site of serum-transferrin; c_1 and c_2, analytical protein and competing ligand concentrations, respectively; μ, ionic strength; oT′, ovotransferrin in interaction with bicarbonate in an unknown state of charge and protonation; oT_NFe, oT_CFe, HoT_NFe, H_2oT_NFe, HoT_CFe, H_2oT_CFe, HoT_CFeL and H_2oT_CFeL, the different kinetic intermediates of the N-site and C-site iron-loaded ovotransferrin in an unknown state of charge and protonation and after bicarbonate loss; H_2oT_N, H_3oT_C and H_4oT_C the N-site and C-site of apo-ovotransferrin in acidic media in an unknown state of charge and protonation; L, the competing ligand in an indefinite structure; $citr^{3-}$, citrate or tricarboxylic acid anion.

(Received 18 February 1999, revised 20 May 1999, accepted 27 May 1999)

$$sT'_NFe + H \leftrightharpoons H_2sT_NFe + HCO_3^- \quad (1)$$

$$H_2sT_NFe + H \leftrightharpoons H_3sT_NFe \quad (2)$$

$$H_3sT_NFe \leftrightharpoons H_3sT_N + Fe \quad (3)$$

$$sT'_CFe + H \leftrightharpoons H_3sT_CFe + H_2CO_3 \quad (4)$$

$$H_3sT_CFe \leftrightharpoons Fe + H_3sT_C \quad (5)$$

$$H_3sT_C + H \leftrightharpoons H_4sT_C \quad (6)$$

$$L + H_3sT_CFe \leftrightharpoons H_3sT_CFeL \quad (7)$$

$$H_3sT_CFeL + H \leftrightharpoons FeL + H_4sT_C \quad (8)$$

Where sT'_N and sT'_C are the iron-loaded N- and C-sites of serum–transferrin in interaction with bicarbonate in an undefined state of protonation, H_2sT_NFe and H_3sT_CFe are the N- and C-site of serum-transferrin after bicarbonate loss and L is the competing ligand in an undefined state.

In this mechanism, we showed that iron is first released from the N-site. This release is triggered by the proton-assisted loss of bicarbonate from the N-site (Eqn 1), which is followed by the proton-assisted loss of Fe(III) (Eqns 2 and 3). At pH $<$ 4, Fe(III) loss from the C-site is triggered by the proton-assisted loss of bicarbonate and by the protonation of the C-site bicarbonate-free iron-loaded protein (Eqns 4 and 6). In addition, at pH $>$ 4, a ternary complex intermediate between competitive chelator L and the iron-loaded protein becomes involved in metal release (Eqns 7 and 8). This mechanism was partly confirmed by X-ray crystallography of the N-site of serum-transferrin [5,14].

As has already been shown, serum-transferrin is an iron-transport system and is known to deliver its load of iron in acidic endosome; the same is expected for ovotransferrin which is also an iron-transport and scavenging system in birds [4]. In a recent series of articles, we examined the mechanisms of iron uptake by human serum-transferrin, bovine lactoferrin and hen ovotransferrin and showed that the uptake of iron by hen ovotransferrin and bovine lactoferrin occurs much more slowly than by serum-transferrin. We also showed that the affinities of the three proteins for Fe(III) are in the same range of magnitude which implies that the metabolic function of a transferrin as an iron-transport or iron scavenging agent in neutral media is more related to kinetics than to thermodynamics. The iron scavengers ovotransferrin and lactoferrin can keep their load of iron much longer than the iron-deliverer serum-transferrin [9,15,16]. In acidic media, lactoferrins behave differently from serum transferrins, as they are known to keep their iron-load even at pH levels as low as 2 [17]. As a result, we expected the iron-deliverer ovotransferrin to behave more like serum-transferrin. Therefore, in this article, we analyse the mechanism of iron release by ovotransferrin by means of the methods and techniques of chemical relaxation [18,19].

MATERIALS AND METHODS

Holo-ovotransferrin and the C-site iron-loaded ovotransferrin were prepared from ovotransferrin (Sigma) and were purified by dialysis according to published procedures [13,20]. Protein concentrations were checked spectrophotometrically [13] and the degree of iron saturation was checked by polyacrylamide/urea gel electrophoresis [20].

KCl and sodium citrate (Merck Suprapur), NaOH, and HCl (Merck Titrisol), EDTA (Merck Titriplex), $FeCl_3$, sodium carbonate (Prolabo Normapur), sodium formate, sodium acetate and sodium citrate (Merck), nitrilotriacetic acid ($NAcH_3$) and Hepes (Aldrich), glycerol, urea and boric acid (Sigma), acrylamide and APS (Ultra Pur, BRL), bromophenol blue (BioRad), Coomassie blue (Biowittaker, France) and *N*,*N*,*N*′,*N*′-tetramethylethylenediamine and Temed (Promega), gaseous CO_2 (Air Liquide, Paris, France, type N45) were used without further purification. Water and glassware were treated as described previously [6].

Stock solutions

All stock solutions were used fresh. Ionic strengths (μ) were adjusted to a final value of 0.2 M with KCl. The sodium formate or acetate concentrations varied from 20–100 mM, whereas those of sodium citrate ranged from 1–10 mM. Final pH values were adjusted with microquantities of concentrated HCl and NaOH. Transferrin concentrations (c_1) ranged from 0.8–125 μM. In order to avoid the formation of $Fe(OH)_3$, the pH was never allowed to exceed 5 with acetate [21]. The situation is different with citrate, where the iron chelate is thermodynamically preferred to $Fe(OH)_3$ [21,22]. Furthermore, the weak formate ligand was only used in acidic media (pH $<$ 4) where there is no risk of $Fe(OH)_3$ formation [23]. A CO_2 controlled atmosphere was obtained in a glove bag or in a special device equipping the stopped flow spectrometer both under continuous flow of a controlled mixture of CO_2 and N_2, delivered by CO_2 and N_2 flow-meters (Aalborg). The solutions were kept under these conditions for two hours before the start of the experiments.

pH measurements

pH values were measured at 25 ± 0.5 °C with a Jenco pH-meter equipped with an Ingold calomel/glass combined microelectrode. Buffers used for pH standardization were pH 7.00 and 10.01 (Sigma).

Spectrophotometric measurements

Spectrophotometric and fluorimetric measurements were performed on a Perkin Elmer lambda 2 spectrophotometer equipped with a magnetic stirring device and on an Aminco-Bowman series 2 luminescence spectrometer, respectively. Both were equipped with a thermostated cell carrier with the sample cell at 25 ± 0.1 °C.

Stopped-flow measurements

Fast kinetic measurements were performed with or without a controlled CO_2 atmosphere on an SF 3 L Hi-Tech stopped-flow spectrophotometer equipped with a thermostated bath at 25 ± 0.5 °C, by mixing iron-saturated or unsaturated transferrin with the acetate, formate or citrate buffers as described previously [12]. The apparatus was equipped with two independent light sources and monochromators. The first was a Deuterium light source and a High-Tech monochromator. This was used for absorption measurements. The second was used for fluorescence detection, and consisted of a 150-W Xenon Mercury lamp (Anovia) associated with a Jarrel-Ash monochromator and a quartz optical fibre. The fluorescence excitation wavelength was set at 280 nm and the emission was acquired via a 320-nm low-cut optical filter. This made it

possible to lower c_1 from ≈ 50 μM to 1 μM in the mixing chamber.

Mathematical formalism and signal analysis

The experimental conditions were set so as to permit the use of chemical relaxation formalism [24]. All experimental signals were analysed as describe elsewhere [6]. They all were pure mono- or multiexponentials and were dealt with as relaxation modes [18,19].

RESULTS

All results are reported at an ionic strength of $\mu = 0.2$. However, in order to test the salt or ionic strength effect on iron release from ovotransferrin [1,25], some experiments were performed at ionic strengths varying from 0.1 to 0.5, with KCl concentrations varying from 50 to 400 mM. The results were identical to those obtained at $\mu = 0.2$. Therefore, under our experimental conditions, the salt effect was not observed.

When a solution of holo-ovotransferrin is submitted to a fast pH jump from neutral to acidic conditions in the presence of citrate, acetate or formate ions, six kinetic processes can be observed in a time range of < 5 ms to 5000 s (Fig. 1). Some of these experiments were performed under variable partial pressure of CO_2 and, as for serum-transferrin, they were independent of these partial pressures and therefore of HCO_3^- concentrations. Decreasing the temperature to 5 °C slows these kinetic phenomena considerably and allows an accurate measurements of the absorption spectra and the trapping of the kinetic intermediates before the beginning of the subsequent process. The pH values of the solutions containing each one of the kinetic intermediates were afterward raised from acidic to neutral by adding cold basic Hepes/HCO_3^- solutions in order to stabilize the intermediate in neutral media in the apo or the monoferric form. Polyacrylamide/urea gel electrophoresis was then performed to identify the state of iron load [20]. All the observed kinetic phenomena, besides the fastest, appear as exponential decreases in absorption in the 400–500 nm range or increases in the fluorescence intensity when the excitation

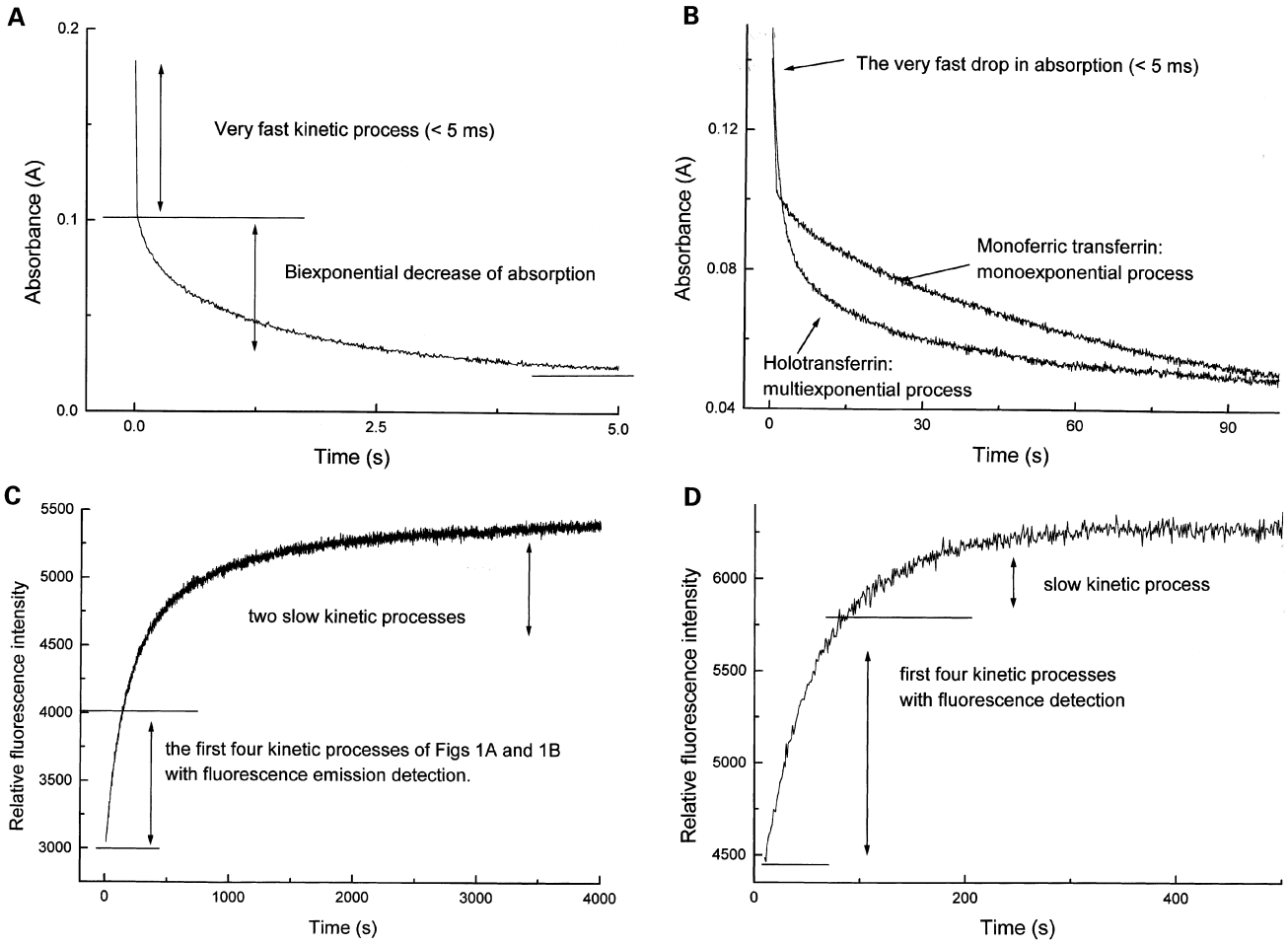

Fig. 1. Decrease in absorption at 465 nm and increase in the fluorescence intensity at an emission wavelength (λ_{em} = 330 nm) for an excitation wavelength (λ_{ex} = 280 nm) subsequent to a rapid pH-jump from neutral (pH 7.40) to acidic (3.2 ≤ pH ≤ 5.6) performed on a holo- or monoferric ovotransferrin. Reported at 25 ± 0.1 °C and $\mu = 0.2$. (A) Biexponential decrease following a very fast drop in absorption, observed with holo-ovotransferrin in the presence of acetate for pH = 3.45, c_1 = 56.8 μM and c_2 = 25 mM (B) The monoexponential decrease following a fast drop in absorption, observed with monoferric-ovotransferrin in the presence of acetate and the triexponential decrease observed with the holoproptein with pH = 4.39, c_1 = 55 μM and c_2 = 25 mM. (C) Multiexponential increase in the fluorescence intensity, observed with holo-ovotransferrin in the presence of acetate at pH = 4.71, c_1 = 1.05 μM and c_2 = 50 mM. (D) Multiexponential increase in the fluorescence intensity, observed with holo-ovotransferrin in the presence of citrate at pH = 5.20, c_1 = 1.24 μM and c_2 = 3 mM.

wavelength is set at λ_{ex} = 280 nm. The amplitude of the fastest process is always observed whether the protein is in the holo- or the monoferric form and depends only on the initial protein concentration (c_0) for pH < 5 (Fig. 1). This amplitude is, however, very weak when detected by fluorescence emission spectroscopy (data not shown). This very fast phenomenon occurs within the limits of the stopped-flow mixing time (Fig. 1A,B). The second and third processes are only detected with the holo-ovotransferrin in the 200 ms to 10 s range (Fig. 1A). All the other kinetic phenomena are observed with both holo and monoferric ovotransferrin. The fourth process occurs in the 10–100 s range and only depends on the pH (Fig. 1B). The fifth process occurs in the 100–1000 s range, its rate being dependent on pH and independent of acetate or formate concentration (Fig. 1C). However, this process depends on citrate concentration with at least a tenfold increase in the overall rate (Fig. 1D). The sixth process occurs in the 1000–5000 s range. It is mainly observed with acetate or formate and depends only on pH (Fig. 1C). With citrate, the amplitude of this process becomes too low to allow its analysis (Fig. 1D). Furthermore, the amplitude of these two final processes becomes negligible at pH < 4. As the state of charge of the different protein species involved in this work is not known charges will not be written.

The first process

The first process of Fig. 1. is too fast to be analysed and, the rates and amplitudes of all the other observed kinetic processes are independent of the CO_2 partial pressures. It was, therefore, assumed that this fast phenomenon may describe proton-assisted decarbonation of the protein in acidic media, because this decarbonation is a prerequisite for iron release [13,14].

$$oT'Fe_2 + nH \leftrightharpoons oTFe_2 + CO_2/(HCO_3)^- \quad (9)$$

where $oT'Fe_2$ is the holo–protein in interaction with bicarbonate and $oTFe_2$ the decarbonated protein. Both are in an unknown state of protonation.

The second and third kinetic processes

The second and third kinetic processes of Fig. 1A are only observed with the holo-ovotransferrin as also shown in Fig. 1B. Both phenomena are directly pH-dependent. The kinetic product which accumulates at the end of the third process is a monoferric ovotransferrin, as confirmed by polyacrylamide gel electrophoresis. These two processes are therefore ascribed to the release of iron from the N-site of the protein. If we assume that this release occurs in a similar manner to that for serum-transferrin with, however, the involvement of two proton transfers instead of a single one for serum-transferrin [13], we can write Equations (10–12):

$$oT_NFe + H^+ \underset{k_{-1}}{\overset{k_1}{\leftrightharpoons}} HoT_NFe \text{ (fast)} \quad (10)$$

$$HoT_NFe + H^+ \underset{k_{-2}}{\overset{k_2}{\leftrightharpoons}} H_2oT_NFe \text{ (slow)} \quad (11)$$

$$H_2oT_N + Fe \leftrightharpoons H_2oT_NFe \text{ (constantly equilibrated)} \quad (12)$$

with $K_{1a} = [H^+][oT_NFe]/[HoT_NFe]$, $K_{2a} = [H^+][HoT_NFe]/[H_2oT_NFe]$ and $K_N = [H_2oT_N][Fe]/[H_2oT_NFe]$

The reciprocal relaxation time equations associated with Eqn (10), the second kinetic process of Fig. 1A, and Eqn (11), the third kinetic process of Fig. 1A, can be expressed as Eqns (13) and (14), respectively [13,19].

$$(\tau_1)^{-1} = k_1[H^+] + k_{-1} \quad (13)$$

$$(\tau_2)^{-1} = k_2[H^+]^2/(K_{1a} + [H^+]) + k_{-2} \quad (14)$$

A very good linear least-squares regression of the experimental data related to the second kinetic process against Eqn (13) is obtained (Fig. 2). From the slope and intercept, $k_1 = (2.30 \pm 0.10) \times 10^4\ M^{-1}\cdot s^{-1}$, $k_{-1} = (1.40 \pm 0.10)\ s^{-1}$ and $K_{1a} = k_{-1}/k_1 = (60 \pm 6)\ \mu M$ are determined.

Another very good linear least-squares regression of the experimental relaxation times related to the third kinetic process against Eqn (14) is obtained (Fig. 3). From the slope and intercept we determine: $k_2 = (5.2 \pm 0.15) \times 10^3\ M^{-1}\cdot s^{-1}$, $k_{-2} = (0.2 \pm 0.02)\ s^{-1}$ and $K_{2a} = k_{-2}/k_2 = (39 \pm 5)\ \mu M$.

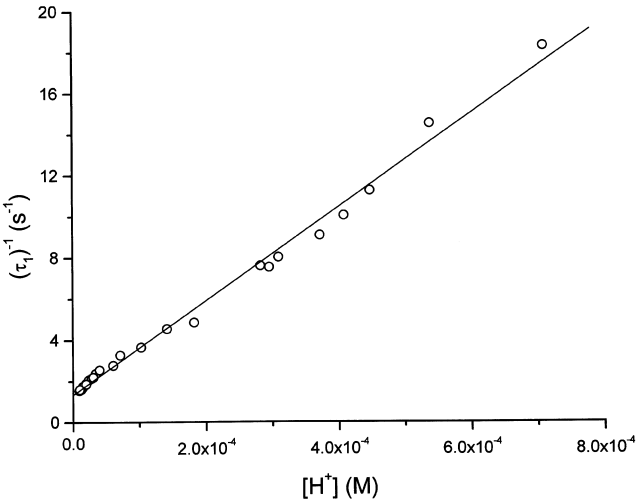

Fig. 2. Plot of $(\tau_1)^{-1}$ against $[H^+]$. Reported for 27 experimental points obtained at 25 ± 0.5 °C, μ = 0.2, 5.0 μM ≤ c_1 ≤ 61.30 μM and 3.15 ≤ pH ≤ 5.31. Intercept (1.40 ± 0.10) s^{-1}; slope (2.30 ± 0.10) × 10^4 $M^{-1}\cdot s^{-1}$ and r = 0.99646.

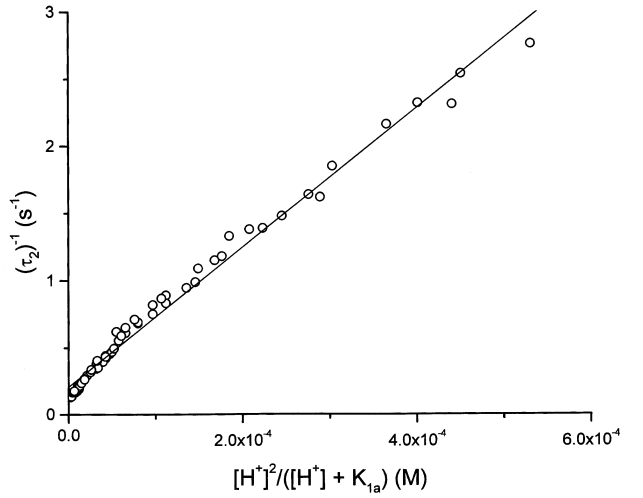

Fig. 3. Plot of $(\tau_2)^{-1}$ against $[H^+]^2/([H^+] + K_{1a})$. Reported for 65 experimental points obtained at 25 ± 0.5 °C, μ = 0.2, 5.0 μM ≤ c_1 ≤ 61.30 μM and 3.15 ≤ pH ≤ 5.31. Intercept (0.20 ± 0.02) s^{-1}; slope (5.20 ± 0.15) × 10^3 $M^{-1}\cdot s^{-1}$ and r = 0.99403.

The fourth kinetic process

For pH > 4, at the end of the fourth process of Fig. 1B–D and before the beginning of the fifth process, the ovotransferrin is still in the monoferric form. This was confirmed by PAGE. The experimental reciprocal relaxation times associated with this fourth process (Fig. 1B–D) depend on nothing other than pH and seem to obey only Eqn (15) (Fig. 4).

$$(\tau_3)^{-1} = k_3[H^+] + k_{-3} \quad (15)$$

Equation (15) is typically associated with a bimolecular acid-base like proton transfer [Eqn (16)] [18,19].

$$oT_CFe + H^+ \underset{k_{-3}}{\overset{k_3}{\rightleftharpoons}} HoT_CFe \quad (16)$$

with $K_{3a} = [oT_CFe][H^+]/[HoT_CFe]$

From the slope of the best linear regression of Fig. 4, we determine $k_3 = (1.22 \pm 0.03) \times 10^3$ M^{-1}·s^{-1}.

The fifth kinetic process

With citrate, $[(\tau_4)^{-1}]$ the experimental reciprocal relaxation times related to the fifth kinetic process in the presence of citrate (Fig. 1D) depend on $[H^+]^2$ and on [L] (Fig. 5, L is citrate concentration, $[L] \gg c_1$, $[H^+]$), whereas with acetate or formate, the experimental reciprocal relaxation times $[(\tau_5)^{-1}$, Fig. 1C] become very short and depend only on pH. The experimental reciprocal relaxation times associated with both processes are independent of c_1, which precludes rate-limiting iron loss from the protein [18,19]. With serum-transferrin, these rates depend on pH and the nature of the ligand, but never on its concentration, and relate to slow proton transfers occurring with the mixed protein-ligand complex (Eqns 7 and 8) [13]. This, and the facts that formate and acetate scarcely complex Fe(III) [23], that citrate is a strong Fe(III) chelator [22], that with acetate or formate the experimental $(\tau_5)^{-1}$ depend on nothing else but pH and that with citrate they depend on $[H^+]^2$ and [L] (Fig. 5), led us to propose Eqns (17–19). In these equations, it was assumed that with the strong citrate ligand, the fifth kinetic process (Fig. 1D) describes a slow proton-transfer following the interaction of the monoferric protein with L, whereas with acetate and formate (Fig. 1C) this kinetic process only relates to a proton transfer.

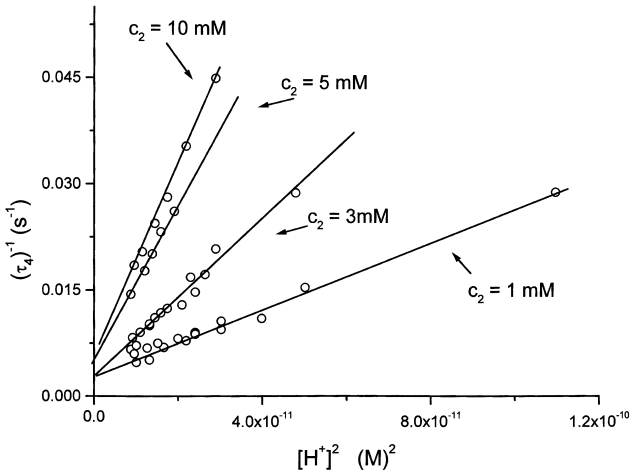

Fig. 5. Plot of $(\tau_4)^{-1}$ against $[H^+]^2$. Reported for 41 experimental points in the presence of citrate obtained for four fixed c_2 1 mM, 3 mM, 5 mM and 10 mM with, 0.5 μM ≤ c_1 ≤ 1.5 μM and 4.98 ≤ pH ≤ 5.53 at 25 °C and μ = 0.2.

$$HoT_CFe + L \underset{k'_{-4}}{\overset{k'_4}{\rightleftharpoons}} HoT_CFeL \quad (17)$$

$$HoT_CFeL + H^+ \underset{k_{-4}}{\overset{k_4}{\rightleftharpoons}} H_2oT_CFeL \text{ (rate-limiting with citrate)} \quad (18)$$

$$HoT_CFe + H^+ \underset{k_{-5}}{\overset{k_5}{\rightleftharpoons}} H_2oT_CFe$$

(rate-limiting with acetate or formate) (19)

with $K_{4a} = [HoT_CFeL][H^+]/[H_2oT_CFeL]$, $K_{LC} = [HoT_CFe][L]/[HoT_CFeL]$ and $K_{5a} = [HoT_CFe][H^+]/[H_2oT_CFe]$.

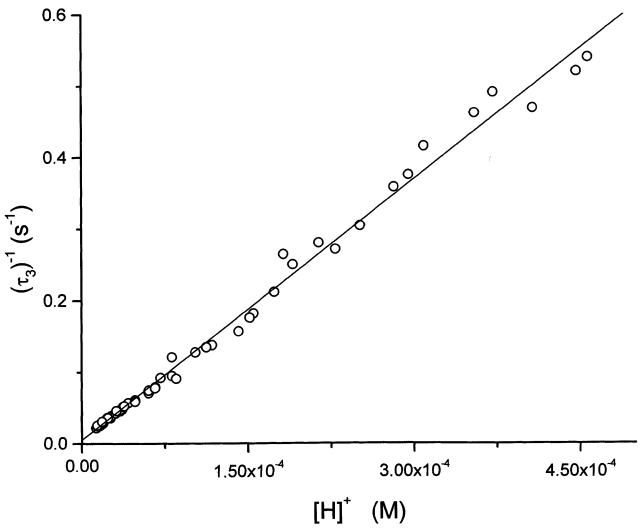

Fig. 4. Plot of $(\tau_3)^{-1}$ against $[H^+]$. Reported at 25 °C for 54 experimental points obtained at 25 ± 0.5 °C, μ = 0.2, 3.27 ≤ pH ≤ 4.89 and 5 μM ≤ c_1 ≤ 65 μm. Intercept (6 ± 6) × 10^{-2}·s^{-1}; slope (1.22 ± 0.03) × 10^3 M^{-1}·s^{-1} and r = 0.99607.

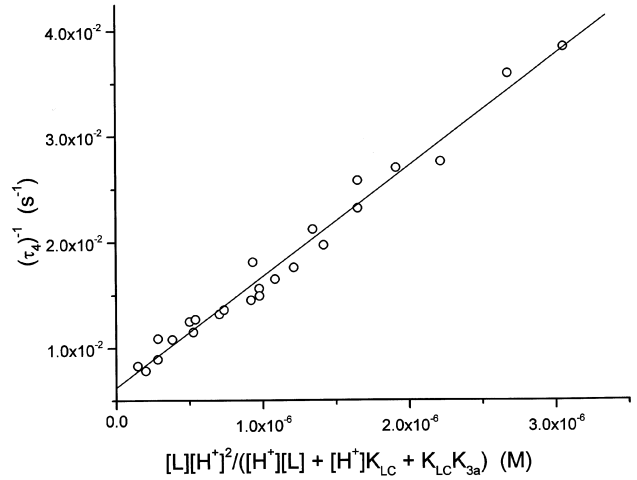

Fig. 6. Plot of $(\tau_4)^{-1}$ against $[H^+]^2[L]/([H^+][L] + [H^+]K_{LC} + K_{LC}K_{3a})$. Reported for 24 experimental points in the presence of citrate obtained for four fixed pH values: 5.15, 5.28, 5.36 and 5.43 with, 0.5 mM ≤ c_2 ≤ 5 mM and 0.5 μM ≤ c_1 ≤ 2 μM at, 25 ± 0.5 °C and μ = 0.2. Intercept (1.0 ± 0.1) × 10^{-2}·s^{-1}; slope (1.05 ± 0.05) × 10^4 M^{-1}·s^{-1} and r = 0.98942.

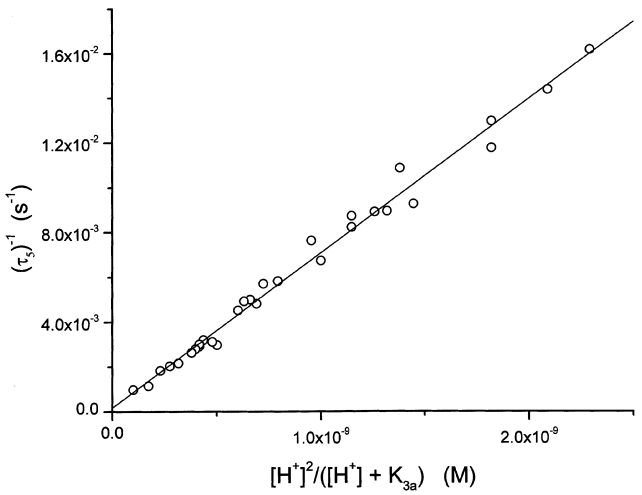

Fig. 7. Plot of $(\tau_5)^{-1}$ against $[H^+]^2/([H^+] + K_{3a})$. Reported for 30 experimental points in the presence of formate or acetate obtained at 25 ± 0.5 °C and $\mu = 0.2$ for $4.30 \leq pH \leq 5.0$, $0.5\ \mu M \leq c_1 \leq 12\ \mu M$ and $10\ mM \leq c_2 \leq 50\ mM$. Intercept $(2 \pm 3) \times 10^{-4}\cdot s^{-1}$; slope $(6.90 \pm 0.30) \times 10^6\ M^{-1}\cdot s^{-1}$ and $r = 0.99396$.

Equations (20–22) can be associated to Eqns (17–19), respectively, when each is rate-limiting (see Appendix).

$$(\tau'_4)^{-1} = k'_4[L]([H^+] + K_{4a})/([H^+] + K_{3a}) + k'_{-4}K_{4a}/[H^+] \quad (20)$$

$$(\tau_4)^{-1} = k_4[H^+]^2[L]/([H^+][L] + [H^+]K_{LC} + K_{LC}K_{3a}) + k_{-4} \quad (21)$$

$$(\tau_5)^{-1} = k_5[H^+]^2/(K_{3a} + [H^+]) + k_{-5} \quad (22)$$

Equation (20) can be discarded because it is never followed by our experimental data. Therefore, Eqn (17) is not rate-limiting. In Eqn (21), we lack the K_{LC} value and were not able to determine K_{3a}. We therefore used a programme in which K_{LC} and K_{3a} varied in the 1 μM to 1 mM range, for each pair of values a linear regression of the data with least squares adjustments against Eqn (21) was performed. The pair of equilibrium constants which led to the best regression line was $K_{LC} = (0.435 \pm 0.015)$ mM and $K_{3a} = (1.00 \pm 0.10)$ mM. Four new series of experiments were then performed at four fixed pH values with c_2 varying from 0.5 to 5 mM (c_2 is the analytical ligand concentration). A good linear least-squares regression of these data against Eqn (21) was obtained (Fig. 6). The slope and intercept of the best line gave: $k_4 = (1.05 \pm 0.05) \times 10^4\ M^{-1}\cdot s^{-1}$, $k_{-4} = (1.0 \pm 0.1) \times 10^{-2}\cdot s^{-1}$ and $K_{4a} = k_{-4}/k_4 = (0.95 \pm 0.15)$ μM.

With acetate and formate and in the absence of citrate, a very good linear least-squares regression of the data against Eqn (22) is obtained (Fig. 7). From the slope of the best line $k_5 = (6.90 \pm 0.30) \times 10^6\ M^{-1}\cdot s^{-1}$ is determined.

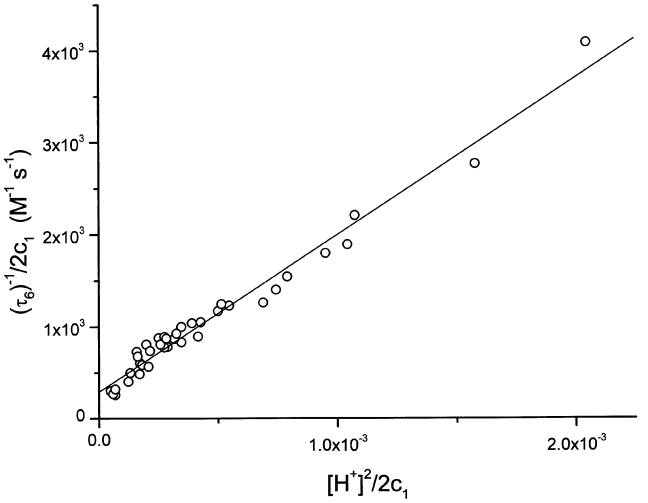

Fig. 8. Plot of $(\tau_6)^{-1}/2c_1$ against $[H^+]^2/2c_1$. Reported for 38 experimental points in the presence of formate or acetate obtained at 25 ± 0.5 °C and $\mu = 0.2$ for $4.30 \leq pH \leq 5.0$, $0.5\ \mu M \leq c_1 \leq 15\ \mu M$ and $10\ mM \leq c_2 \leq 50$ mM. Intercept $(290 \pm 60)\ M^{-1}\cdot s^{-1}$; slope $(1.70 \pm 0.10) \times 10^6\ M^{-1}\cdot s^{-1}$ and $r = 0.98663$.

The sixth kinetic process

At the end of the final kinetic process (Fig. 1), the protein becomes iron-free. The amplitude of this last process becomes too low to allow any kinetic analysis in the presence of citrate (Fig. 1D), whereas with formate and acetate (Fig. 1C), the rates depend on pH. As for serum-transferrin, this last process can be ascribed to a slow protonation [13], Eqns (23–25).

$$H_2oT_CFe + H^+ \underset{k_{-6}}{\overset{k_6}{\rightleftharpoons}} H_3oT_CFe \text{ (rate-limiting)} \quad (23)$$

$$H_3oT_C + Fe \rightleftharpoons H_3oT_CFe \quad (24)$$

$$Fe + L \rightleftharpoons FeL \quad (25)$$

with $K_{6a} = [H_2oT_CFe][H^+]/[H_3oT_CFe]$, $K_C = [H_3oT_C][Fe]/[H_3oT_CFe]$ and $K_{FeL} = [Fe][L]/[FeL]$.

The reciprocal relaxation time equation when Eqn (23) rate-limiting is expressed under our experimental conditions ($4.2 \leq pH \leq 5.2$ and $c_2 \gg c_1$ when $K_{5a} > 0.1$ mM [13]), as Eqn (26) (Appendix).

$$(\tau_6)^{-1} = k_6[H^+]^2/K_{5a} + k_{-6}2c_1/K_C \quad (26)$$

which can also be expressed as:

$$(\tau_6)^{-1}/2c_1 = k_6[H^+]^2/(K_{5a}2c_1) + k_{-6}/K_C \quad (27)$$

A very good linear least-squares regression of the data against Eqn (27) is obtained (Fig. 8). From the slope of the best regression line, $k_6/K_{5a} = (1.70 \pm 0.10) \times 10^6\ M^{-1}\cdot s^{-1}$, $k_{-6}/K_C = (290 \pm 60)\ M^{-1}\cdot s^{-1}$.

DISCUSSION

To avoid citrate-Fe(III) complex polymerization, all experiments with citrate were performed at $c_2 \leq 10$ mM [26]. Citrate also exists in acidic media as four different prototropic species, $citr^{3-}$, $Hcitr^{2-}$, H_2citr^- and H_3citr, with $K_{7a} = [H^+][citr^{3-}]/[Hcitr^{2-}] = 0.41$ μM, $K_{8a} = [H^+][Hcitr^{2-}]/[H_2citr^-] = 17.0$ μM and $K_{9a} = [H^+][H_2citr^-]/[H_3citr] = 72.4$ mM. Therefore, in order to have a single major citrate species in the medium, our experiments were performed at $5 \leq pH \leq 5.5$ where, $[H_3citr] \ll [Hcitr^{2-}] \geq 0.70c_2$. This, however, does not exclude intermediate complex formation between iron-loaded ovotransferrin and $citr^{3-}$ and or H_2citr^-. Indeed, when a ligand loses a proton its affinity for the metal increases, sometimes to such an extent that complex formation occurs with the

nonprotonated species at pH values where the free ligand is still in the protonated form [27,28].

Citrate species concentrations can be determined from Eqns (28–30) [9].

$$[citr^{3-}] = K_{7a}K_{8a}c_2/([H^+]^2 + [H^+]K_{8a} + K_{7a}K_{8a}) \quad (28)$$

$$[Hcitr^{2-}] = [H^+]K_{8a}c_2/([H^+]^2 + [H^+]K_{8a} + K_{7a}K_{8a}) \quad (29)$$

$$[H_2citr^-] = [H^+]^2c_2/([H^+]^2 + [H^+]K_{8a} + K_{7a}K_{8a}) \quad (30)$$

The replacement of [L] by $[citr^{3-}]$ in the equation associated with the mechanism of intermediate complex formation [Eqn (21)] is not obeyed by the experimental data. On the other hand, the replacement of [L] by $[Hcitr^{2-}]$ in the same equation does not affect our results whereas that of [L] by $[H_2citr^-]$ is still followed by the experimental data. We can therefore assume that $[citr^{3-}]$ is not involved in the intermediate complex formation between ovotransferrin and citrate.

In Table 1, we summarize the mechanisms of iron loss by serum-transferrin and ovotransferrin. The differences between iron release from ovotransferrin and from serum-transferrin seem important. However, a thorough analysis of both mechanisms clearly indicates that the two proteins have similar but not identical behaviours toward Fe(III) loss in acidic media. They differ in the rates of iron release, the number of proton transfers involved and the rate-limiting steps. Nevertheless, in both proteins, proton-assisted carbonate loss seems to be the indispensable trigger for iron release [13]. This is confirmed by an X–ray diffraction study on the N-site of serum-transferrin [14]. With serum-transferrin, the release of the metal from the N-site involves a single slow proton-transfer reaction which we ascribed to an acid-base reaction occurring on the Hist ligand (Eqn 2) and probably controlled by the change of conformation from close to open occurring upon iron loss [12,16]. This was also confirmed by X-ray diffraction [5]. With ovotransferrin, iron release from the N-site occurs in two steps, each of which involves a slow proton transfer [Eqns (10) and (11)]. As for serum-transferrin, no intermediate complex between the holoprotein and the competing ligands present in the medium is observed during iron release from the N-site [13]. With the C-site, the mechanism of iron release seems much more complex with ovotransferrin than with serum-transferrin. Nevertheless, the two mechanisms obey the same rules with some differences in the proton uptakes, in the rates and in the rate-limiting steps. In very acidic media ($2.5 < pH < 3.5$), with serum-transferrin the loss of iron is kinetically controlled by a slow proton transfer (Eqn 6), which probably occurs on the Asp ligand of the apoprotein [12]. This probably describes the change in conformation of the lobe from the iron-containing closed structure to the iron-free opened conformation [13]. At $pH > 3.5$, an intermediate complex between the competing ligands present in the medium and the monoferric C-site is formed (Eqn 7). The rates of iron release from this intermediate are controlled by a slow proton transfer, as shown in Eqn (8), [13]. With ovotransferrin, after the fast proton assisted decarbonation (Eqn 9), the first step in iron release from the C-lobe is a slow proton transfer (Eqn 16), followed by two possible paths, each of which depends on the strength of the competing ligand (Eqns 17–19 and 23). In the presence of a strong iron chelator such as citrate [22], the C-site iron-loaded protein forms an intermediate complex with the ligand (Eqn 17). Iron loss is then controlled by what appears to be a slow proton uptake by the intermediate complex (Eqn 18). In contrast, with very weak ligands such as formate or acetate [23], no intermediate complex seems to be formed. In this case, iron loss becomes controlled by what appears to be a very slow

Table 1. The general mechanism of iron loss by ovotransferrin and serum-transferrin.

	Ovotransferrin			Serum-transferrin		
Reaction	Second order rate constant ($M^{-1}\cdot s^{-1}$)	First order rate constant (s^{-1})	pK	pK	Second order rate constant ($M^{-1}\cdot s^{-1}$)	Reaction
$oT'Fe_2 + nH \leftrightharpoons oTFe_2 + CO_2/(HCO_3)^-$	–	–	–			$sT'_NFe + H \leftrightharpoons H_2sT_NFe + HCO_3$
$oT_NFe + H^+ \underset{k_{-1}}{\overset{k_1}{\leftrightharpoons}} HoT_NFe$	2.3×10^4	1.40	5.22		7.40×10^4	$H_2sT_NFe + H \leftrightharpoons H_3sT_NFe$
$HoT_NFe + H^+ \underset{k_{-2}}{\overset{k_2}{\leftrightharpoons}} H_2oT_NFe$	5.20×10^3	0.2	4.40			
$H_2oT_NFe \leftrightharpoons H_2oT_NFe$	–	–	–			$H_3sT_NFe \leftrightharpoons H_3sT_N + Fe$
				–	2.25×10^4	$sT'_CFe + H \leftrightharpoons H_3sT_CFe + H_2CO_3$
$oT_CFe + H^+ \underset{k_{-3}}{\overset{k_3}{\leftrightharpoons}} HoT_CFe$	1.22×10^3	–	4.00	–	–	
$HoT_CFe + L \leftrightharpoons HoT_CFeL$	–	–	3.35	–	–	$L + H_3sT_CFe \leftrightharpoons H_3sT_CFeL$
$HoT_CFeL + H^+ \underset{k_{-4}}{\overset{k_4}{\leftrightharpoons}} H_2oT_CFeL$	1.05×10^4	1.00×10^{-2}	6.00	–	1.75×10^3	$H_3sT_CFeL + H \leftrightharpoons FeL + H_4sT_C$
$HoT_CFe + H^+ \underset{k_{-5}}{\overset{k_5}{\leftrightharpoons}} H_2oT_CFe$	6.90×10^6	–	–			
$H_2oT_CFe + H^+ \leftrightharpoons H_3oT_CFe$	–	–	–			
$H_3oT_C + Fe \leftrightharpoons H_3oT_CFe$	–	–	–			$H_3sT_CFe \leftrightharpoons Fe + H_3sT_C$
$H_3oT_C + H^+ \leftrightharpoons H_4oT_C$				4	4.25×10^3	$H_3sT_C + H \leftrightharpoons H_4sT_C$
$Fe + L \leftrightharpoons FeL$						$Fe + L \leftrightharpoons FeL$

proton gain by a monoferric protein [Eqn (19)]. This can imply that this essential metal-loaded protein proton gain is favoured by the formation of the intermediate ternary complex with citrate. With serum-transferrin, iron-loss in the presence of citrate is faster than with formate or acetate. However, in this last case, the reciprocal relaxation times are independent of citrate concentration. This can be explained by the fact that the reciprocal relaxation time [Eqn (21)] associated with the slow proton transfer in the presence of citrate can be simplified in Eqn (31) when the affinity of citrate ligand for the decarbonated monoferric protein is high ($K_{LC} \ll [H^+]$, [L]).

$$(\tau_4)^{-1} = k_4[H^+] + k_{-4} \quad (31)$$

The rate is then independent of ligand concentration but dependent on the nature of the ligand involved in the intermediate complex formation [13]. Therefore, iron release from the C-site of ovotransferrin occurs by a mechanism similar to that for serum-transferrin with, however, lower rates and the involvement of an additional proton transfer. This additional proton transfer can be due to the discrepancies in the interdomain H-bonds which exist in each of the iron-binding clefts of the two proteins [29]. These H-bonds can break upon protonation of the amino acids involved rendering the metal more accessible to the outside medium [9]. Nevertheless, in transferrins, Fe(III) is co-ordinated to the same protein ligand in a practically identical environment [2–4,29]. Despite this fact, the behaviour of the transferrins towards iron loss is not identical, as it is slower with ovotransferrin than with serum-transferrin and occurs in very acidic media with lactoferrin [13,17]. The co-ordination bonds with a transition metal are always several orders of magnitude stronger than any classical H-bond [28,30]. We therefore believe that the central metal constitutes the nucleus, which maintains the two domains of each lobe in a particular geometry. Interdomain H-bonds can help to reinforce this particular conformation or may control by their position the access to the metal. This can apply to holo-lactoferrins interdomain H-bonds involving nonprotonable amino-acid side-chains [29] which can retard the opening of the binding cleft and iron loss in acidic media. This can also apply to the dilysine interdomain H-bond in the N-site of ovotransferrin, which is positioned at the lips of the binding cleft [31]. Its protonation can break this H-bond, rendering the metal more accessible to the extra-proteic medium.

Acid-base reactions are diffusion-controlled proton transfers, which occur in the μs range [18,19]. The slow proton transfer observed during iron loss from transferrins can therefore be rate-controlled by the dynamic change in the conformation of the protein from closed to open which can manifest by a transition of the apparent pK_as of amino acids engaged in the closed conformation, to their thermodynamic values in the opened conformation [9]. Most of the 'acid-base like' pK_as reported in Table 1 are close to those of the side-chains of the amino acids involved in complex formation between ovotransferrin and Fe(III) and in the interdomain H-bonds present in the C-binding cleft. We can therefore cautiously speculate that after the loss of carbonate, the first step involved in iron release form the C-site of ovotransferrin is the protonation of one of the Glu or Asp engaged in the interdomain H-bonds [Eqn (16), pK_a = 4]. This allows the interaction of the competing citrate ligand with the co-ordination sites of the metal left accessible by carbonate loss. This is followed by the protonation of the imidazole of the Hist ligand [Eqn (18), pK_{4a} = 6]. In the absence of citrate, iron loss occurs at lower pH values and does not involve the formation of the intermediate ternary complex.

CONCLUSIONS

We have here shown that the iron scavenging and transport system ovotransferrin loses iron in acidic media by a mechanism similar to that of the pure iron transport system serum-transferrin, and does not behave in a manner similar to that of the scavenging agent lactoferrin, which is known to keep its Fe(III) at very low pH values [17]. However, in neutral media ovotransferrin does behave as the iron-scavenging lactoferrin [9,16]. This may explain the duality of ovotransferrin as an iron scavenger in neutral media and/or deliverer in acidic endosomes. However, our results are reported *in vitro* and cannot be easily transposed in endosomes, where iron loss occurs from the protein in interaction with its specific receptor.

APPENDIX

The substitution method was used to derive the reciprocal relaxation time equations, Eqns (20),(21),(26) and (27) [18,19].

Derivation of Eqn (20)

The conservation of mass and the constant state of equilibrium of Eqns (16) and (17) and the rate-control by Eqns (18) and (16) allow us to write,

$$-d[H_2oT_CFeL]/dt = k'_{-4}[HoT_CFeL] - k'_4[HoT_CFe][L] = 0 \quad (34)$$

$$\Delta[oT_CFe] + \Delta[oT_CHFe] + \Delta[oT_CHFeL] + \Delta[oT_CH_2FeL] = 0 \quad (35)$$

$$\Delta[L] + \Delta[oT_CHFeL] + \Delta[oT_CH_2FeL] = 0 \quad (36)$$

$$\Delta[HoT_CFe] = [H^+]\Delta[oT_CFe]/K_{3a} + [oT_CFe]\Delta[H^+]/K_{3a} \quad (37)$$

$$\Delta[H_2oT_CFeL] = [H^+]\Delta[HoT_CFeL]/K_{4a} + [HoT_CFeL]\Delta[H^+]/K_{4a} \quad (38)$$

From Eqns (34–38), Eqn (20) is derived.

Derivation of Eqn (21)

When Eqn (18) is rate-limiting, we can write,

$$-d[H_2oT_CFeL]/dt = k_4[H_2oT_CFeL] - k_{-4}[H^+][HoT_CFeL] \quad (39)$$

$$\Delta[HoT_CFeL] = [HoT_CFe]\Delta[L]/K_{LC} + [L]\Delta[HoT_CFe]/K_{LC} \quad (40)$$

Eqn (21) was derived from Eqns (35),(36),(39) and (40).

Derivation of Eqn (22)

In the absence of citrate, if Eqn (19) is rate-limiting, we can write,

$$-d[H_2oT_CFe]/dt = k_{-5}[H_2oT_CFe] - k_5[HoT_CFe][H^+] \quad (41)$$

$$\Delta[oT_CFe] + \Delta[HoT_CFe] + \Delta[H_2oT_CFe] = 0 \quad (42)$$

Eqn (22) was determined from Eqns (37), (41) and (42).

Derivation of Eqns (26) and (27)

The conservation of mass, the constant state of equilibrium of Eqns (24) and (25) and rate-control by Eqn (23) allow us to write,

$$-\mathrm{d}[H_3oT_C]/\mathrm{dt} = k_{-6}[H_3oT_CFe] - k_6[H^+][H_2oT_CFe] \quad (43)$$

$$\Delta[H_2oT_CFe] + \Delta[H_3oT_CFe] + \Delta[H_3oT_C] = 0 \quad (44)$$

$$\Delta[L] + \Delta[FeL] = 0 \quad (45)$$

$$\Delta[FeL] + \Delta[H_2oT_CFe] + \Delta[H_3oT_CFe] = 0 \quad (46)$$

$$\Delta[H_3oT_CFe] = [Fe]\Delta[H_3oT_C]/K_C + [H_3oT_C]\Delta[Fe]/K_C \quad (47)$$

$$\Delta[FeL] = [L]\Delta[Fe]/K_{FeL} + [Fe]\Delta[L]/K_{FeL} \quad (48)$$

Under our experimental conditions, $[L] \gg c_1$, K_{FeL}.

Equation (26) is derived from Eqns (43–48).

ACKNOWLEDGEMENT

The authors are grateful to P. Levoir for writing the computer programmes used in this work.

REFERENCES

1. Aisen, P. (1998) Transferrins, the transferrin receptor, and the uptake of iron by cells. In *Metal in Biological Systems* (Sigel, A. & Sigel, H., eds), Vol. 35, pp. 585–665. Marcel Dekker, New York.
2. Anderson, B.F., Baker, H.M., Norris, G.E., Rice, D.W. & Baker, E.N. (1989) Structure of human lactoferrin – crystallographic structure analysis and refinement at 2.8 Å resolution. *J. Mol. Biol.* **209**, 711–734.
3. Zuccola, H.J. (1992) *The crystal structure of monoferric human serum transferrin*. PhD Thesis (Georgia Institute of Technology) UMI, Ann Arbor.
4. Kurokawa, H., Mikami. B. & Hirose, M. (1995) Crystal structure of diferric hen ovotransferrin at 2.4 Å resolution. *J. Mol. Biol.* **254**, 196–207.
5. Jeffrey, P.D., Bewley, M.C., MacGillivray, R.T., Mason, A.B., Woodworth, R.C. & Baker, E.N. (1998) Ligand-induced conformational change in transferrins, crystal structure of the open form of the N-terminal half of human transferrin. *Biochemistry* **37**, 13978–13986.
6. El Hage Chahine, J.M. & Fain, D. (1993) The mechanism of iron–transferrin interactions – uptake of the iron nitrilotriacetic acid complex. *J. Chem. Soc. Dalton Trans*. 3137–3143.
7. Bellounis, L., Pakdaman, R. & El Hage Chahine, J.M. (1996) Apotransferrin proton dissociation and interactions with bicarbonate in neutral media. *J. Phys. Org. Chem.* **9**, 111–118.
8. Pakdaman, R. & El Hage Chahine, J.M. (1997) Transferrin – the interaction of lactoferrin with hydrogen carbonate. *Eur. J. Biochem.* **249**, 149–155.
9. Bou Abdallah, F. & El Hage Chahine, J.M. (1998) Transferrins – hen-ovotransferrin – interaction with bicarbonate and iron uptake. *Eur. J. Biochem.* **258**, 1022–1031.
10. Baker, E.N. & Lindley, P.F. (1992) New perspectives on the structure and function of transferrins. *Inorg. Biochem.* **47**, 147–160.
11. Dautry-Varsat, A., Cienchanover, A. & Lodish, H.F. (1983) pH and recycling of transferrin during receptor-mediated endocytosis. *Proc. Natl Acad. Sci. USA* **80**, 2258–2262.
12. El Hage Chahine, J.M. & Fain, D. (1994) The mechanism of iron release from transferrin – slow proton induced loss of nitrilotriacetatoiron (III) complex in acidic media. *Eur. J. Biochem.* **223**, 581–587.
13. El Hage Chahine, J.M. & Pakdaman, R. (1995) Transferrin, a mechanism for iron release. *Eur. J. Biochem.* **230**, 1101–1110.
14. MacGillivray, R.T., Moore, S.A., Chen, G., Anderson, B., Baker, H., Luo, Y., Bewley, M., Smith, C.A., Murphy, M.E.P., Wang, Y., Mason, A.B., Woodworth, R.C., Brayer, G.D. & Baker, E.N. (1998) Two high-resolution crystal structures of the recombinant N-lobe of human transferrin reveal a structural change implicated in iron release. *Biochemistry* **37**, 7919–7928.
15. Pakdaman, R. & El Hage Chahine, J.M. (1996) A mechanism for iron uptake by transferrin. *Eur. J. Biochem.* **236**, 922–931.
16. Pakdaman, R., Petitjean, M. & El Hage Chahine, J.M. (1998) Transferrins – a mechanism for iron uptake by lactoferrin. *Eur. J. Biochem.* **254**, 144–153.
17. Montreuil, J., Tonnelat, J. & Mullet, S. (1960) Préparation et propriétés de la lactosidérophiline du lait de femme. *Biochim. Biophys. Acta.* **45**, 413–421.
18. Eigen, M. & DeMaeyer, L. (1963) Relaxation methods. In *Techniques of Organic Chemistry – Investigation of Rates and Mechanism of Reactions, part II* (Freiss, S.L., Lewis, E.S. & Weissberger, A., eds), Vol. 8, pp. 895–1029. Wiley Interscience, New York.
19. Bernasconi, C.F. (1976) *Relaxation Kinetics*. Academic Press, New York.
20. Makey, D.G. & Seal, U.S. (1976) The detection of four molecular forms of human transferrin during the iron-binding process. *Biochim. Biophys. Acta* **453**, 250–256.
21. Martell, A.E. & Smith, R.M.S. (1989) *Critical Stability Constants*, Vol. I. Plenum Press, New York.
22. Field, T.B., McCourt, J.L. & McBryde, W.A.E. (1974) Composition and stability of iron and copper citrate complexes in aqueous solutions. *Can. J. Chem.* **52**, 3119–3124.
23. Tsubota, H. (1962) Formation constants of some metal formate complexes, and the use of formate buffer solution as an elutriant for cation-exchange chromatography. *Bull. Soc. Chem. Japn.* **35**, 640–644.
24. Brouillard, R. (1980) How much an equilibrium can be shifted in a chemical relaxation experiment. *J. Chem. Soc. Faraday Trans. I* **76**, 583–587.
25. Williams, J., Chasteen, N.B. & Moreton, K. (1982) The effect of salt concentration on the iron-binding properties of human transferrin. *Biochem. J.* **201**, 527–532.
26. Spiro, T.G., Bates, G. & Saltman, P. (1967) The hydrolytic polymerization of ferric citrate. II. The influence of excess citrate. *J. Am. Chem. Soc.* **89**, 5559–5562.
27. Hancock, R.D. & Martell, A.E. (1989) Ligand design for selective complexation of metal ions in aqueous solutions. *Chem. Rev.* **89**, 1875–1914.
28. Wilkins, R.G. (1976) *The Study of Kinetics and Mechanism of Reactions of Transition Metal Complexes*. Allyn and Bacon, Boston.
29. Moore, A.S., Anderson, B.F., Groom, C.R., Haridas, M. & Baker, E.N. (1997) Three-dimensional structure of diferric bovine lactoferrin at 2.8 Å resolution. *J. Mol. Biol.* **274**, 222–2236.
30. Zundel, G. (1976) Easily polarizable hydrogen bonds – their interaction with the environment – IR continuum and anomalous large proton conductivity. In *The Hydrogen Bond* (Schuster, P., Zundel, G. & Sandorfy, C., eds), pp. 683–766. Elsevier, New York.
31. Dewan, J.C., Mikami, B., Hirose, M. & Sacchettini, J.C. (1993) Structural evidence for pH-sensitive trigger in the hen ovotransferrin N-lobe. Implication for transferrin iron release. *Biochemistry* **32**, 11963–11968.